OPTICAL MATERIALS

Optical materials have emerged as an extremely important class of materials in the modern world. From simple mirrors in everyday use to complex optical communication systems using lasers, optical fibers, and photodetectors, optical materials have gained a unique position in the advancement of technology. A number of optical properties such as refractive index, absorption coefficient, nonlinear dielectric susceptibility,

and their variations with respect to applied electric and magnetic fields are exploited in a variety of applications. These applications include ferroelectric oxides as electro-optic modulators, semiconductors as light sources and detectors, polymers as holographic optical storage devices and image processing devices, and glass as an optical fiber. However, future optical materials will largely be in the form of optical coatings, i.e., thin and thick films of optical materials designed and fabricated to suit particular applications.

FERROELECTRICS

Ferroelectrics have nonlinear optical properties that are exploited for a number of applications. These nonlinear properties are attributed to (1) crystalline structure lacking a center of inversion symmetry, (2) large nonlinear susceptibilities, and (3) large spontaneous birefringence. Electro-optic modulators have been successfully fabricated in several materials, such as barium titanate ($BaTiO_3$), lithium titanate ($LiTiO_3$), and lead zirconium titanate (PLZT ceramics) (1). The PLZT compositions contain 9% or more lanthanum and are called *slim-loop* materials because they have negligible remanent polarization. These electro-optic modulators have applications in industrial and military eye protection devices, stereoscopic three-dimensional television, and one-dimensional optical memories. At present, titanium-diffused bulk lithium niobate ($LiNbO_3$) channel waveguide structures are the most widely used optical modulators because of their relative ease of fabrication (2). Figure 1 shows optical-grade $LiNbO_3$ boules and wafers of 7.5 cm to 10 cm (3 in. to 4 in.) diameter grown by the Czochralski technique. The waveguides are characterized by low propagation losses (usually in the range of 0.1 to 0.2 dB/cm) and exhibit very low coupling losses (0.5 dB/facet). In practical modulators the optical properties should not degrade when subjected to a light beam and a radio-frequency field. Certain materials, such as strontium barium niobates ($Sr_{1-x}Ba_xNb_2O_6$), have extremely large electro-optic coefficients, but their properties degrade in the presence of modulation fields (3). Both potassium hydrogen phosphate (KH_2PO_4, KDP) and potassium deuterium phosphate (KD_2PO_4, DKDP) are widely used as modulator materials, but both of them are hygroscopic and require a water-free environment for their operation (3). Table 1 gives a number of ferroelectric materials and their optical properties.

Figure 1. Lithium niobate boules and wafers (2).

SEMICONDUCTORS

Semiconductors are the backbone of the modern electronics industry. The electronic properties of semiconductors are of utmost importance in the design and fabrication of integrated circuits used in computers, video games, and electronic instruments. On the other hand, the optical properties of semiconductors, such as their emission and absorption characteristics, are used extensively in light sources and detectors for optical communication systems. Semiconductors are also used as solar cell materials to convert the sun's light into electricity and as optoelectronic integrated circuit materials. Figure 2 shows a number of semiconductors with their energy bandgaps and their corresponding wavelengths of emission. As seen in this figure, the compound semiconductor gallium arsenide (GaAs) emits at a wavelength of 0.85 μm, one of the useful wavelengths for light sources used in optical communication. The transmission windows for silica fibers (the wavelengths at which the losses and dispersion are a minimum in silica fibers) are at 0.85, 1.30, and 1.55 μm. Since there are no elemental or compound semiconductors that emit radiation at 1.30 and 1.55 μm, it has become necessary to employ ternary and quaternary III–V alloys to produce materials of appropriate bandgaps. However, the choice of materials is limited by the fact that high-quality epitaxial materials can be grown only on those substrates that have a lattice match to the grown material. Since gallium arsenide (GaAs) and indium phosphide (InP) substrates are available readily, the ternary and quaternary alloys such as aluminum gallium arsenide (AlGaAs) and indium gallium arsenide phosphide (InGaAsP) are grown on GaAs and InP respectively. In spite of the good lattice match between GaAs and AlAs, the thermal expansion coefficients of GaAs and AlGaAs differ substantially, resulting in dislocations at the interface during cooling. However, very efficient luminescent devices (light-emitting diodes and lasers) radiating in the range 0.8 μm to 0.9 μm are fabricated of materials in the AlGaAs–GaAs system and are used as light sources in optical communication systems, compact disc players, and pointing devices. The details on the design and fabrication of these devices can be found in the excellent Refs. 4 to 8.

Light Detection Devices

In a receiver set of an optical communication system, the light signal is converted to an electrical signal. The detection devices used for this purpose are usually photoconductors or photodiodes. Silicon photodiodes are commonly used to detect the light from GaAs–AlGaAs laser sources at 0.85 μm. Here the absorption coefficient of the material, α, determines the thickness of the semiconductor to be used. The absorption coefficient of silicon is of the order of 10^3 cm^{-1} requiring at least 50 μm thick material. For optical detection at 1.30 μm and 1.55 μm wavelengths heterojunction photodiodes are more commonly used. In this case, a large-bandgap semiconductor such as InP is used as a substrate material, and smaller-bandgap alloys such as gallium indium arsenide (GaInAs)

Table 1. Ferroelectric Materials and Their Properties

Material	Static Dielectric Constant	Electro-Optic Constants (pm/V)	Refractive Index
$BaTiO_3$ (barium titanate)	3600	$r_{42} = \begin{cases} 1640\,(\text{unclamped}) \\ 820\,(\text{clamped}) \end{cases}$	2.49
$LiNbO_3$ (lithium niobate)	$\epsilon_3 = 32$ $\epsilon_1 = 78$	$r_{33} = \begin{cases} 30.8\,(\text{clamped}) \\ 34.0\,(\text{unclamped}) \end{cases}$	2.29
ADP (ammonium dihydrogen phosphate)	56	8.5	1.53
KDP (KH_2PO_4) (potassium dihydrogen phosphate)	$\epsilon_3 = 21$ $\epsilon_1 = 42$	$r_{63} = -10.5$ $r_{41} = 8.6$	1.51
DKDP (potassium dideuterium phosphate)	$\epsilon_3 = 50$	$r_{63} = 26.4$ $r_{41} = 8.8$	1.51
$Ba_2NaNb_5O_{15}$ (barium sodium niobate)	51	36	
$Sr_{0.75}Ba_{0.25}Nb_2O_6$ (strontium barium niobate)	750	$r_{33} = 1340$	2.31
$LiTaO_3$ (lithium tantalate)	$\epsilon_3 = 45$ $\epsilon_1 = 51$	$r_{33} = 30.3$	2.18
PLZT (lead zirconium titanate)	—	102 to 612	—

and GaInAsP are grown epitaxially on InP. Detailed information on heterojunction photodiodes can be found in Refs. 9 and 10. Photoconductors are used in detecting visible (0.4 μm to 0.7 μm) and infrared (0.7 μm to 1 mm) radiations. In these devices, the conductivity of the material is altered by the photon irradiation and is detected as a photocurrent. Cadmium sulfide (CdS), with an energy bandgap of 2.42 eV, has a very high sensitivity at about 0.5 μm in the visible region of the spectrum. To improve the gain of this photoconductor, effective trap states for holes are introduced using dopants such as iodine or chlorine. The detection sensitivity of a CdS photoconductor can be extended to higher wavelengths of the visible spectrum by adding copper to create trap states in the bandgap of the material to allow absorption of low-energy photons. Such detectors in the visible range find applications in illumination-level measuring instruments, in exposure meters for cameras, and as control devices to switch light on and off inside a home by measuring the light intensity. Narrow-bandgap semiconductors such as Ge (E_g = 0.67 eV), InSb (E_g = 0.18 eV), PbSe (E_g = 0.27 eV), and PbS (E_g = 0.41 eV) can be used as photoconductors in the near infrared range (0.7 μm to 2 μm). The Ge devices are typically operated at liquid nitrogen temperature (77 K) to reduce thermal noise.

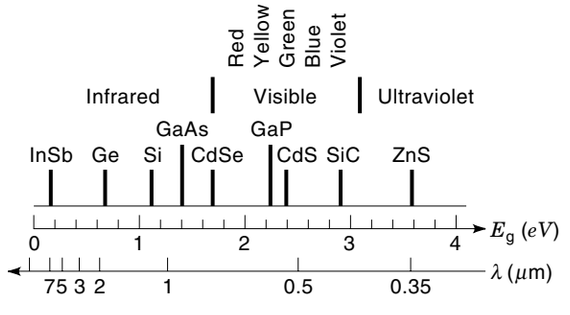

Figure 2. Bandgaps of some common semiconductors relative to the optical spectrum (10).

For the detection of mid-infrared radiation (2 μm to 10 μm), ternary alloys of II–VI compounds such as HgCdTe can be fabricated with appropriate bandgaps. However, the crystal growth technology of these alloys with well-controlled stoichiometry (appropriate ratios of elements in an alloy) is yet to be realized (11). To obtain photoconductors to detect very long wavelengths (10 μm to 100 μm), germanium doped with gallium, silicon doped with phosphorus, and GaAs doped with selenium or tellurium are commonly used. Again these materials have to be operated at low temperatures (77 K) to ensure that the free carriers are not excited from the impurity levels by thermal energies. Lastly, infrared radiation in the range 0.1 mm to 1 mm is detected with free electron absorption. Such devices are cooled to liquid helium temperature (4 K).

Solar cells, or photovoltaic devices that convert light energy into electrical energy, use a wider range of semiconducting materials than any other optical device. The most important optical properties of solar cell materials are (1) absorption coefficient, (2) energy bandgap, and (3) quantum efficiency, defined as the number of electron–hole pairs generated per incident photon.

Two important parameters of a solar cell are V_o, the open-circuit voltage, and I_s, the short-circuit current. The maximum efficiency of a solar cell is obtained by maximizing the output power, which is typically 80% of the product V_oI_s. Hence, considerable research effort has gone into the design

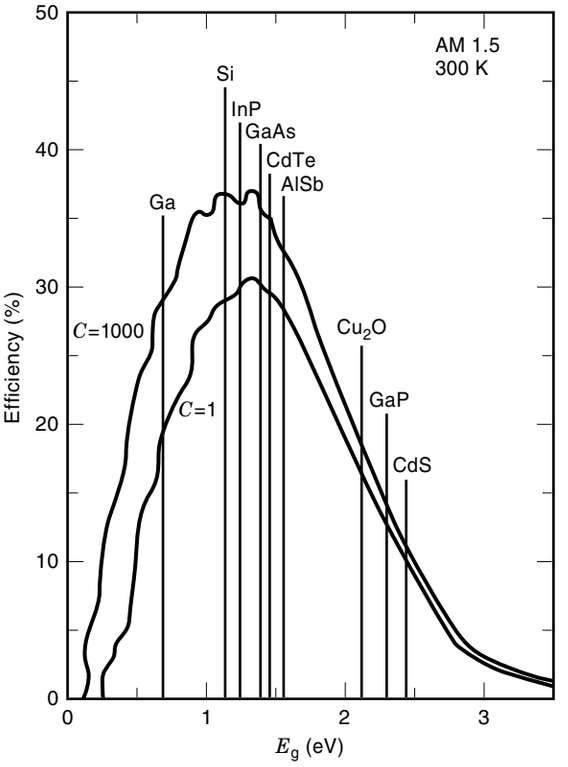

Figure 3. Ideal solar cell efficiency at 300 K for 1 sun and for 1000 sun concentration (10).

of solar cells and choice of materials to achieve large values of V_o and I_s simultaneously. Again, *pn* junctions are the obvious choice for devices, and semiconductors are the best choice for materials. The dependence of the solar cell efficiency on the energy bandgap of a semiconductor is shown in Fig. 3. A maximum efficiency of about 28% occurs around 1.4 eV to 1.5 eV, corresponding to the bandgaps of Cu_2S, InP, GaAs, and CdTe. Because of the low material costs and availability of advanced technology, silicon solar cells are most commonly used today.

One important material consideration in the fabrication of solar cells is to obtain highly pure starting materials devoid of metallic impurities such as chromium, copper, iron, and sodium, which degrade the minority carrier lifetime, thus reducing I_s. On the other hand, the stringent material requirements (e.g., the crystal quality) needed in the fabrication of integrated circuits can be relaxed in the manufacture of solar cells. Large-grain polycrystalline and amorphous silicon are extensively used to reduce the material costs in manufacturing solar cells. Mass production of polycrystalline silicon ribbons and sheets has been accomplished by dendritic web growth or edge-defined film-fed growth or chemical vapor deposition.

A 10% efficient solar cell can provide roughly 100 W/m^2 in a sunny location. In order to obtain higher power it is possible to use solar concentrator systems where 100 or even 1000 times the sun's actual energy flux can be incident on the cell, using mirrors and lenses. Although silicon cells are not very suitable (their efficiency decreases with increasing temperature due to concentrated sunlight), GaAs and GaAs–AlGaAs heterojunction solar cells can withstand temperatures up to 100 °C. Comprehensive reviews on photovoltaic materials are found in Refs. 4, 10, 12, and 13.

Optoelectronic Integrated Circuits

Like electronic monolithic integrated circuits, optoelectronic monolithic integrated circuits with lasers, modulators, photodetectors, and electronic components all on a single chip have been fabricated, and limited success has been achieved in the actual implementation of these chips. One of the major hurdles in high-speed computing is the delay in the electrical interconnects. If photons instead of electrons are used to carry the message from one device to another device on the chip or from one chip to another chip in a microprocessor system, the speed of the system can be significantly enhanced. Photons are preferred over electrons because they are not subject to propagation delays caused by the finite resistance, capacitance, and inductance of the interconnects. The optical materials being developed for optical waveguides to replace electrical interconnects are GaAs–AlGaAs, InP–GaAsP, photorefractive materials, and certain organic materials having nonlinear effects. Details on optoelectronic integrated circuits can be found in Refs. 7, 14, and 15.

Multiple-Quantum-Well Structures

With the availability of computer-controlled molecular beam shutters in molecular beam epitaxy (MBE) systems since the early 1980s, it has been possible to grow extremely thin (1 nm to 5 nm) layer-by-layer structures in a variety of III–V and II–VI semiconducting alloys such as GaAs–AlGaAs, GaInAs–AlInAs, GaSb–GaAlSb, GaInAs–InP, CdTe–CdMnTe, GaAsSb–GaAlSb, and ZnSe–ZnMnSe (16). Quantum well lasers constructed of alternate layers of GaAs and AlGaAs of thicknesses of a few nanometers have better spontaneous quantum efficiency than conventional double heterojunction lasers made of GaAs and AlGaAs. This results in a reduction of the threshold current density and its temperature dependence. Recently, a few more semiconducting optical material systems have gained significant importance. They are: (1) porous silicon (17), (2) gallium nitride (GaN) and related compounds (18), (3) Si–Ge alloys (19), (4) diamond (20), (5) silicon carbide (SiC) (21), and wide-bandgap II–VI semiconductors (22).

GLASS

Glass is one of the most important optical materials, used in many applications, including optical fibers to transmit information across continents, lenses to improve the vision of millions of people, and a variety of display devices. As one of the most widely used manufactured materials, glass is used in everyday life (mirrors, telescopes, electric light bulbs, buildings, bottles and tumblers for drinking, and cookware). A few other interesting applications of glass are found in nose cones of missiles, crowns for teeth, beads in human organs to help them tolerate radiation doses, and even in nuclear waste disposal.

Glass is essentially an inorganic liquid with the rigidity of a solid. Glass has a number of unique properties, e.g., it is transparent and durable, it can be shaped to different forms

easily, and it is inexpensive. The use of glass in fiber optics and liquid crystal displays is a 16 billion dollar industry in the US (23). Tempered glass produced using a chemical process rather than by quick cooling can withstand pressures up to 150 MPa (22,000 lb/in.^{2}) (23). This special glass is used in eyeglasses, oven cookware, basketball backboards, and car windows. Lead oxide (PbO) and barium oxide (Ba_2O_3) are added to the basic sand–soda–lime (SiO_2–Na_2CO_3–CaO) mixture to obtain sparkling glass, boric oxide (B_2O_3) is added to obtain heat-resistant glass, and chromium (Cr) and copper (Cu) are added to make green sunglasses. Certain other oxides such as aluminum oxide (Al_2O_3) add durability to glass, magnesium oxide (MgO) reduces the melting temperature, boric oxide (B_2O_3) reduces the viscosity, and lead oxide (PbO) increases the refractive index (23,24). The refractive index of a glass can be varied from 1.517 for borosilicate glass to 1.980 for phosphate glass by adding different oxides. Corning manufactures 750 different glasses and glass related products. Notable among these are Macor, machinable glass used to make glass nuts and bolts and window frames for the Space Shuttle, and Dicor, used in dental crowns that are plaque-resistant and highly translucent.

Optical Fibers

Long-distance transmission of optical signals requires low-loss optical fibers to maximize the distance between repeaters. Apart from the wavelength of the optical signal (the loss is only 0.2 dB/km at 1.55 μm, but 0.5 dB/km at 1.30 μm), the purity of the silica (SiO_2) used in the construction of the fiber determines the losses of the signal. Glasses containing less than 1 ppm of transition metal ions have attenuations as low as 0.2 dB/km. Figure 4 shows the attenuation in optical fibers as a function of wavelength. As indicated already, low transmission losses occur at 1.30 μm and 1.55 μm. Another important aspect of the choice of wavelength of transmission is the dispersion of the fiber. Dispersion is the variation of the refractive index of the optical fiber with wavelength.

When material absorption and dispersion are reduced to a minimum at $\lambda = 1.55$ μm by proper variation of the refractive index of the fiber, Rayleigh scattering, which is due to the granularity of silica, dominates the absorption in the medium (25). One way to reduce Rayleigh scattering is to use crystalline materials. Crystalline zirconium fluoride (ZrF), arsenic triselenide ($AsSe_3$), and potassium iodide (KI) have very low attenuations ($\sim 10^{-2}$ dB/km) in the 2 μm to 5 μm range (26). Heavy-metal fluoride glasses (ZrF_2, PbF_2, BaF_2) with low phonon energies and chalcogenide glasses based on sulfides, selenides, and tellurides and their mixtures are being investigated as candidates for optical transmission (27).

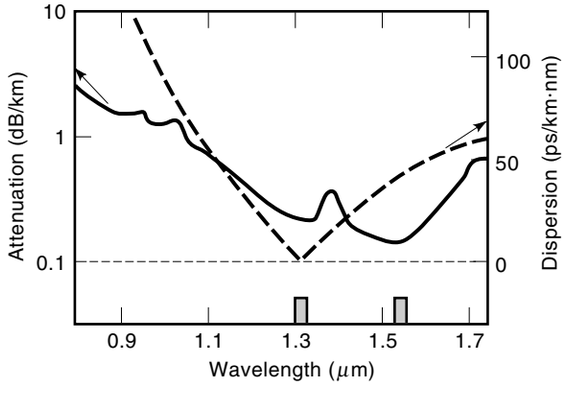

Figure 4. Optical attenuation and dispersion behavior of standard silica fiber (25).

Table 2. Rare Earth Ions Used in Laser Glasses (28)

Ion	Host Glass (Oxides)	λ (μm)
Nd^{3+}	K–Ba–Si	1.060
	La–Ba–Th–B	1.370
	Na–Ca–Si	0.920
	Li–Ca–Al–Si	1.060
Yb^{3+}	Li–Mg–Al–Si	1.015
	K–Ba–Si	1.060
Ho^{3+}	Li–Mg–Al–Si	2.100
Er^{3+}	Yb–Na–K–Ba–Si	1.543
	Li–Mg–Al–Si	1.550
	Yb–Al–Zn–P	1.536
Tm^{3+}	Li–Mg–Al–Si	1.850
	Yb–Li–Mg–Al–Si	2.105

Optical Amplifiers

Instead of using electronic amplifiers at repeater stages to boost the signal strength, modern optical communication systems use amplifiers made of silica optical fiber doped with erbium (Er^{3+}). These amplifiers can be laser-diode-pumped at 0.80 μm, 0.98 μm, and 1.48 μm wavelengths. However, this amplifier suffers from a short fluorescence lifetime due to nonradiative decay. Pr^{3+}-doped amplifiers use fluoride glasses as host materials with fluorescence lifetime of 100 μs.

Laser Glasses

The first lasers were made of crystals, e.g., ruby lasers (Al_2O_3 containing Cr^{3+} ions) and YAG lasers ($Y_3Al_5O_{12}$ containing Nd^{3+} ions) emitting at 0.69 μm and 1.06 μm respectively. Table 2 shows the rare earth ions used in various types of glasses and their corresponding emission wavelengths (28). Although Nd^{3+} is the most favored ion in a variety of host glasses, the durability and ease of fabrication favor alkali metal and alkaline earth silicates (28). The main difference between glass lasers and crystal lasers is that large, isotropic, and homogeneous volumes with good optical quality glass lasers can be easily fabricated. Furthermore, the disordered structure of glass allows many more sites for ions to occupy than in ordered structures. However, the spectra of glass lasers contain broader fluorescent lines ($\sim$30 nm) than the spectra of lasers made of crystalline materials (YAG has 1 nm broadening) (28).

POLYMERS

Several nonlinear optical phenomena have been observed in organic materials (29–31). These phenomena include: (1) third-harmonic generation, (2) two-photon absorption, (3) electric-field-induced second-harmonic generation, (4) inten-

Table 3. Figure of Merit for Inorganic and Organic Materials (31)

Material	Electro-Optic Coefficient r (pm/V)	Refractive Index n	Dielectric Constant ϵ	Figure of Merit $Q = n^3r/\epsilon$ (pm/V)
Gallium arsenide (GaAs)	1.430	3.40	12	4.7
Barium titanate	1640	2.49	3600	7.0
Lithium niobate ($LiNbO_3$)	34	2.29	32	12.8
$Sr_{0.75}Ba_{0.25}Nb_2O_6$	216	2.3	750	3.5
Organic crystal	67	2.0	3.2	168
Organic polymer	30	1.6	4.0	31
Photorefractive polymer	3.1	1.7	7.0	2.2

sity-dependent index of refraction, and (5) stimulated Raman scattering.

The major difference between inorganic and organic nonlinear optical materials is the origin of the nonlinearity. In inorganic materials the optical nonlinearity is mainly due to the ionic polarizability resulting from the displacement of the ions. Hence large electro-optic coefficients in materials such as $BaTiO_3$ and $KNbO_3$ are also associated with large dielectric constants. Since the optical nonlinearity and dielectric constant are inextricably linked, the figure of merit (see Table 3) of inorganic materials does not change significantly from one material to the other. On the contrary, in organic materials the optical nonlinearity is a molecular property arising from the asymmetry of the electronic charge distributions in the ground and excited states of the individual molecules. Thus, a large figure of merit (an increase of a factor of ten over inorganics) can be achieved in organic materials.

Another major advantage of organics over inorganics is the ease of fabrication and processing of polymers and their compatibility with integrated circuit processing techniques. The polymers can be easily fabricated in the form of thin films of high optical quality and can be modified by means of chemical doping.

Three main classes of polymers have emerged as the most promising materials in optoelectronics. They are: (1) guest–host systems, (2) side-chain systems, and (3) cross-linked systems (30). In guest–host systems, a nonlinear chromophore is dissolved in a host polymer without any chemical bond between the dye and the polymer. The dye concentration in the polymer determines its optical quality and electro-optic efficiency. Since the dyes are disordered in the host system, a center of symmetry exists and no second-order response is possible. However, the dye molecules can be aligned in an intense static electric field at a temperature above the glass transition temperature of the polymer, and a second-order effect can be generated. Unfortunately, the electro-optic coefficient has so far been less than 10 pm/V. The electro-optic coefficient can be enhanced by creating a chemical attachment or a bond between the dye molecule and the polymer molecule. This can be accomplished either axially (main-chain) or on a side of the polymer molecule (side-chain). The latter configuration has better orientation stability, leading to stable optical properties.

A comparison of the figures of merit of polymers and organics with inorganic materials is given in Table 3 (31). As seen in this table, in spite of low values of electro-optic coefficients, the figures of merit of the polymers can be significantly higher than those of ferroelectric oxides.

One major problem that exists in the development of polymers is their temperature stability and mechanical ruggedness. To date, polymers are used in high-speed modulators, directional couplers, second- and third-harmonic generators, programmable optical interconnects, multiple-image processors and optical data storage systems. A recent issue of the *MRS Bulletin* has articles on polymer electroluminescent devices and conjugated polymer surfaces and interfaces for light-emitting devices (32–34).

OPTICAL PROPERTIES

The principal optical properties of materials are related to the phenomena of absorption, reflection, refraction, transmission, dispersion, polarization, emission, and birefringence. These properties are the (1) refractive index n, (2) complex dielectric function ϵ, (3) extinction coefficient k, (4) absorption coefficient α, (5) reflection coefficient R, (6) transmission coefficient T, (7) electro-optic coefficient r_{ij}, (8) dispersion coefficient d_λ, and (9) Abbe number v_d, which is a measure of the chromatic aberration in an optical material. These optical phenomena and their relationships to the optical properties of materials are described in detail below.

Absorption

When light interacts with matter, the matter may partially absorb the light, partially transmit the light, and partially reflect the light. The proportions of light absorbed A, transmitted T, and reflected R, are essentially determined by the refractive index and extinction coefficient of the material. Our current understanding of this interaction of light with matter is based on Maxwell's equations that describe light as electromagnetic waves. It is the variation of the magnitudes and directions of electric and magnetic field vectors in a medium with respect to space and time that allows us to determine the optical properties of the medium. In a one-dimensional case (assuming that light travels in one direction), the dependence of the electric field phasor on space and time is given as:

$$E = E_0 \exp[\, j\omega(nx/c - t)] \exp\left(-\frac{\alpha x}{2}\right) \tag{1}$$

In this equation, E is the electric field, E_0 the amplitude, ω the frequency, n the real part of the refractive index, c the velocity of light in vacuum, t the time, α the absorption coefficient of the medium, and x the propagation direction. If $\alpha = 0$ (no absorption), the wave propagates without any attenuation in the medium. If $\alpha \neq 0$ (absorbing medium), the intensity of light, I, decays exponentially in the distance x:

$$I = I_0 \exp(-\alpha x) \tag{2}$$

where I_0 is the intensity of light on the surface of the medium. The intensity I is related to the electric field E by $I = E^*E$, where E^* is the complex conjugate of E. The absorption coef-

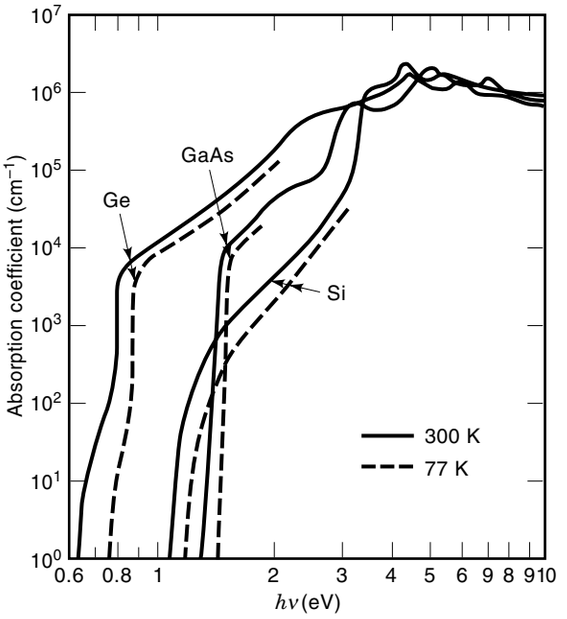

Figure 5. Measured absorption coefficients near and above the fundamental absorption edge for pure Ge, Si, and GaAs (10).

ficient α is related directly to the extinction coefficient as $\alpha = 4\pi k/\lambda$.

Short-Wave Cutoff—Bandgap Effects. The cause of the short-wavelength cutoff in semiconductors, shown in Fig. 5, is the bandgap E_g of the semiconductor. The cutoff wavelength is related to the bandgap by a simple equation

$$\lambda_c = 1.24/E_g \tag{3}$$

where λ_c is the cutoff wavelength in micrometers and E_g the energy bandgap in electron volts. As seen in Fig. 5, λ_c shifts to the left (higher values) as E_g of the material decreases. In degenerately doped semiconductors the lowest energy levels of the conduction band are completely filled. This gives an effective bandgap larger than that of the intrinsic material. The shift in λ_c, known as Burstein–Moss shift, is directly related to the free electron concentration, since the free electrons block the lowest states of the conduction band.

Long-Wave Cutoff—Electron Gas Effects. Longer-wavelength photons of incident radiation are usually absorbed by lattice ions in resonance with incident radiation. However, in metals and conducting oxides the photons interact with the electron gas. Drude developed the theory of this interaction. According to this theory, the complex dielectric function of a medium, ϵ^*, is expressed in terms of the refractive index n and extinction coefficient k as shown below:

$$\epsilon^* = (n - jk)^2 = \epsilon_1 - j\epsilon_2 = \epsilon_\infty - \frac{Nq^2}{\epsilon_0 m_n^*}\left(\omega^2 - \frac{j\omega}{\tau}\right)^{-1} \tag{4}$$

Here ϵ_1 and ϵ_2 are the real and imaginary parts of the dielectric function, ϵ_∞ the static dielectric function, N the free electron concentration, q the electron charge, ϵ_0 the permittivity of free space, m_n^* the effective mass of a conduction electron, and τ the relaxation time. Separating the complex dielectric function into its real and imaginary parts yields

$$\epsilon_1 = n^2 - k^2 = \epsilon_\infty - \frac{Nq^2}{\epsilon_0 m_n^*}\left(\omega^2 + \frac{1}{\tau^2}\right)^{-1} \tag{5}$$

and

$$\epsilon_2 = 2nk = \frac{Nq^2}{\epsilon_0 m_n^* \omega\tau}\left(\omega^2 + \frac{1}{\tau^2}\right)^{-1} \tag{6}$$

The electron gas plasma frequency is defined as the value of ω for which $\epsilon_1 = 0$. Solving Eq. (5) for $\omega = \omega_p$, the plasma frequency, we obtain

$$\omega_p^2 = \frac{Nq^2}{\epsilon_s m_n^*} - \frac{1}{\tau^2} \tag{7}$$

where $\epsilon_s = \epsilon_\infty \epsilon_0$. The electron gas plasma frequency is converted to wavelength in micrometers using

$$\lambda_p = \frac{1.24q}{\hbar\omega_p} \tag{8}$$

Here $\hbar$ is $h/2\pi$, where h is Planck's constant. From Eqs. (7) and (8) it is seen that the plasma wavelength cutoff λ_p depends on the material properties (e.g., ϵ_s, m_n^*, and τ) and the doping properties (e.g., N). The values of m_n^* and τ do depend slightly on the doping concentration.

Reflection

Two important laws govern reflection of light at an interface: (1) the angle of incidence is equal to the angle of reflection, (2) the incident ray, reflected ray, and normal to the interface all lie in the same plane. Based on the classical theory, the reflectivity R of a material having an interface with air (vacuum) under normal incidence conditions is expressed as

$$R = \frac{|\boldsymbol{E}_r|^2}{|\boldsymbol{E}_i|^2} = \frac{(n-1)^2 + k^2}{(n+1)^2 + k^2} \tag{9}$$

where $|\boldsymbol{E}_r|$ and $|\boldsymbol{E}_i|$ are the magnitudes of the reflected and incident electric field vectors respectively. For nonconducting materials ($k = 0$), R given in Eq. (9) reduces to

$$R = \frac{(n-1)^2}{(n+1)^2} \tag{10}$$

For conducting materials the reflection is approximately given as (35)

$$R \approx 1 - \left(\frac{2\omega\epsilon_s}{\pi\sigma}\right)^{1/2} \tag{11}$$

where σ is the conductivity of the material. Hence metals with conductivities of the order of $10^8\ \Omega^{-1}\cdot m^{-1}$ reflect over 90% of the incident light at visible frequencies ($\omega \sim 10^{15}$ rad/s).

Total Internal Reflection. A very interesting phenomenon called total internal reflection occurs whenever light is inci-

dent at an angle greater than the critical angle, θ_c, from a medium of higher refractive index, n_1, into a medium of lower refractive index, n_2. The critical angle, θ_c, is given as:

$$\theta_c = \sin^{-1}(n_2/n_1) \tag{12}$$

This concept is used in guiding light through optical fibers. A cladding material of higher refractive index than that of optical fiber core enables light to be guided along the fiber by total internal reflection mechanism. The details on optical fibers can be found in a section on glass.

Refraction

When electromagnetic waves (light) pass from one medium of refractive index, n_1, to a second medium of refractive index, n_2, the direction and speed of the wavefronts change. This phenomena is known as refraction. According to Snell's law:

$$\sin\theta_i / \sin\theta_r = n_2/n_1 = v_1/v_2 \tag{13}$$

where θ_i is the angle of incidence, θ_r the angle of refraction, v_1 the speed of light in medium 1 (c/n_1) and v_2 the speed of light in medium 2 (c/n_2). Since no refraction occurs in vacuum, its refractive index is set equal to one. The index of refraction of air is 1.0003 and hence it is used as a reference standard to determine the refractive indices of optical materials.

Transmission

The ability to transmit information via optical fibers rather than a metallic cable has revolutionized the modern communication technology. The optical fibers made of silica (SiO_2) have extremely low optical attenuation of less than 0.5 dB/km. The transmission capacity of these fibers is increased by increasing the bit rate ($>10^9$ bits/s). The reflection and transmission coefficients of a material are dependent on the polarization of the light and are given in the next section.

Polarization

Polarization is another important property of light that can be exploited for practical applications. Polarization is defined as the locus of the tip of the electric field vector as a function of time. Depending on the light source and optics involved, light can be linearly polarized (locus is a straight line), circularly polarized (locus is a circle), or elliptically polarized (locus is an ellipse). According as the motion of the tip of the electric field vector is clockwise or counterclockwise, circular and elliptical polarization are described as left-handed or right-handed.

Mathematically, for a wave traveling in the z direction the x and y components of the electric field are given as

$$E_x = E_{01}\cos(\omega t - kz + \phi_a) \tag{14a}$$

$$E_y = E_{02}\cos(\omega t - kz + \phi_b) \tag{14b}$$

Here E_{01} and E_{02} are the amplitudes of E_x and E_y respectively, ϕ_a and ϕ_b are the phases associated with the two components, and k is the magnitude of the wave vector, equal to $2\pi/\lambda$.

The requirement for linear polarization is $\phi_b - \phi_a = 0$ or π radians. In this case the ratio of E_y to E_x is a fixed positive or negative quantity. Circular polarization occurs only if the ratio E_{02}/E_{01} is equal to one and the phase difference $\phi_b - \phi_a = \pm\pi/2$ radians. The wave represented by Eq. (14) is elliptically polarized if it is neither linearly nor circularly polarized.

Many light sources in real life (e.g., sunlight or light from an electric lamp) are unpolarized (randomly polarized). A glare (reflection of sunlight from the surface of water or a sheet of metal) is partially polarized. In the automobile industry, design and implementation of glareless headlight systems has been a major task. Orthogonal polarizations have been considered in the communication industry to double the capacity of a fixed frequency band allocated to a radio or a television station.

Reflection and Transmission Coefficients. The reflection and transmission coefficients are defined for a parallel polarized wave (the direction of electric field vector is parallel to the plane of incidence) and a perpendicularly polarized wave (the direction of electric field vector is perpendicular to the plane of incidence). For a parallel polarized wave they are (36)

$$R_1 = \frac{(n_2/n_1)\cos\theta_i - \cos\theta_t}{(n_2/n_1)\cos\theta_i + \cos\theta_t} \tag{15a}$$

$$T_1 = \frac{[2(n_2/n_1)\cos\theta_i]}{(n_2/n_1)\cos\theta_i + \cos\theta_t} \tag{15b}$$

Here it is assumed that the two media have identical permeabilities ($\mu_1 = \mu_2$). The angles θ_i and θ_t are the angles of incidence and transmission respectively. θ_t is obtained from Snell's law of refraction [Eq. (13)].

Brewster's Angle. For a certain angle of incidence $\theta_i = \theta_b$, called Brewster's angle in the case of a parallel polarized wave, the reflection coefficient R_1 given by Eq. (15a) is zero. For this particular angle of incidence the wave is totally transmitted. This angle is determined by the refractive indices of the two media and is expressed as

$$\theta_b = \tan^{-1}(n_2/n_1) \tag{16}$$

A gas laser fitted with a Brewster's-angle window produces linearly polarized light. Details can be found in Ref. 36. For many optical materials and devices, the polarization of light is important because the polarization state of light is manipulated and controlled by the material properties.

Electronic Polarization. The velocity of a high-frequency electromagnetic wave (visible light) is reduced in a material because of the electronic polarization (electrons respond to the rapidly varying electric and magnetic fields, whereas ions cannot respond). The high-frequency dielectric constant of the material is given by $\epsilon_s = n^2$. It is possible to relate the index of refraction of a crystal to the physical properties of the crystal as shown below (37):

$$\frac{M}{\rho}\frac{n^2-1}{n^2+2} = \frac{N_0\beta}{3\epsilon_0} \tag{17}$$

Here N_0 is the Avagadro's number, M the molecular weight, ρ the density, and β the polarizability of a molecule.

In summary, most materials are polarizable in different ways according to the frequency of the applied electric and

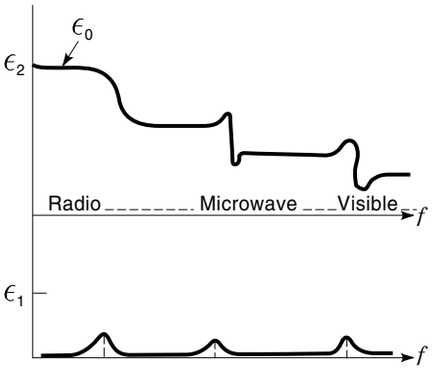

Figure 6. Typical variation of ϵ_1 and ϵ_2 with frequency (26).

magnetic fields. An important medium, water, has $\epsilon_s = 80$ at radio frequencies, but its refractive index is not equal to $(80)^{1/2}$ as expected, but 1.3. At optical frequencies $\epsilon_s \approx 2$, indicating contribution only from the electronic polarization. At low frequencies, the orientational polarization of a water molecule is dominant because the ions respond to the slowly varying fields. Typical variation of the real and imaginary parts of the complex dielectric function given in Eqs. (5) and (6) as a function of frequency is shown in Fig. 6. As seen in this figure, the peaks at different frequencies in ϵ_2 correspond to absorption by the medium due to either orientational or electronic polarizations. A discontinuity observed in ϵ_1 at the same frequencies is also a result of the polarization of the medium. These frequencies correspond to natural resonance frequencies of the system, corresponding to rotational, vibrational, or electronic energy transitions in the system. Materials such as glass that transmit visible light usually absorb strongly in the ultraviolet and infrared regions because of the time difference between the induced and applied fields.

Emission

The general phenomenon of light emission (energy given out) by an electronic transition from a higher energy state to a lower energy state is called luminescence. Depending upon the excitation process, the emission can be photoluminescence (free carriers are excited by photon absorption) or cathodoluminescence (free carriers are excited by high-energy electron bombardment) or electroluminescence (free carriers are excited by passing a current). If the crystal emits light almost simultaneously (within 10^{-8} s), the emission is called fluorescence. At the other extreme, if it takes more than a microsecond to emit light, the emission is called phosphorescence and the materials are called phosphors. In direct bandgap semiconductors such as GaAs, the light emission is fluorescent and the emission wavelength is determined by the bandgap of the material [see Eq. (3)]. In indirect bandgap materials such as zinc sulfide (ZnS), the wavelength of light (i.e., its color) depends on the impurity levels present.

Cathodoluminescence. Display systems such as cathode ray tubes (CRT) in television sets or flat panel display systems in a laptop computer make use of a high-energy electron beam to excite electrons in a phosphor-coated screen. As an example, in color television, the screen is coated with ZnS, a phosphor. The ZnS is doped with different impurities such as Cu, Ag, and Mn to emit the primary additive colors red, green, and blue. Three electron beams are swept together to excite appropriate phosphor dots to produce a broad range of colors by addition of red, green, and blue.

Electroluminescence. Light-emitting diodes (LED) and lasers consist of *pn* diodes where injection of minority carriers by an electric current results in light emission when the minority carriers recombine with the majority carriers. A detailed description of light-emitting semiconductors has been given in the section on semiconductors.

Birefringence

Tetragonal and hexagonal crystals do not have the symmetry of the cubic crystals and hence possess anisotropic properties (the refractive index changes with direction inside the crystal) except for the *c* axis, which is called the optic axis. Ordinary light entering these anisotropic crystals in a direction other than that of the optic axis is split into two linearly polarized beams, which travel through the crystal in different directions. This phenomenon, known as birefringence or double refraction, is observed in many transparent crystals, such as calcite and quartz. As shown in Fig. 7, one ray, called the ordinary ray or *O* ray, traverses the crystal obeying Snell's law, whereas the other ray, called the extraordinary ray or *E* ray, violates Snell's law. Irrespective of the polarization of the incident light, the *E* ray has its electric field variations in a plane containing the optic axis of the crystal and the incident ray. The *O* ray is always polarized in a direction perpendicular to the *E* ray. The velocities of the two rays are different, depending upon the refractive indices in two different directions. Thus, a phase difference of 90° or 180° between the rays can be created by choosing an appropriate thickness of the crystal. This is the basis of electro-optic modulation, described in the next subsection.

Isotropic materials are described by only one relative permittivity, i.e., ϵ_r. The refractive index n is equal to $\epsilon_r^{1/2}$. For anisotropic media, the relative permittivity is a dielectric tensor with nine components. The diagonal terms, ϵ_{r1}, ϵ_{r2}, and ϵ_{r3}, are known as the principal dielectric permittivities. In anisotropic materials, if $\epsilon_{r1} = \epsilon_{r2} \neq \epsilon_{r3}$, the material is called *uniaxial,* whereas if $\epsilon_{r1} \neq \epsilon_{r2} \neq \epsilon_{r3}$, it is called *biaxial.* In uniaxial materials, if $\epsilon_{r3} < \epsilon_{r1}$, the material is said to be negative uniaxial (e.g., $LiNbO_3$), and if $\epsilon_{r3} > \epsilon_{r1}$, the material is said to be positive uniaxial (e.g., quartz, $LiTaO_3$, and TiO_2).

A very interesting application of birefringence is in liquid crystals, used extensively as display devices. There are three types of liquid crystal structures: nematic, cholesteric, and smectic. The molecules of these materials are easily polariz-

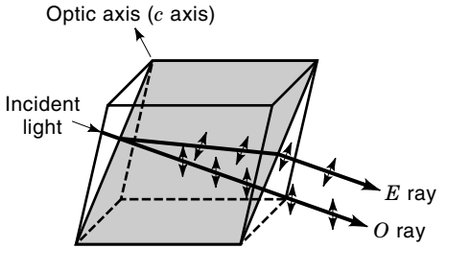

Figure 7. *O* ray and *E* ray inside a crystal (37).

able under the influence of an electric field. By aligning the molecules in an appropriate manner it is possible to either allow light of a particular polarization to pass through (creating a bright spot) or block it (creating a dark spot). Many material- and device-related challenges remain in the development of liquid crystal display devices. Materials that possess low threshold voltages, high nonlinear responses, high stability, high resistivity, and low absorption are being developed.

Electro-Optic Effects

Two important applications of optical materials—high-speed modulators and second-harmonic generators—make use of the electro-optic effects observed in many crystals. There are two electro-optic effects: (1) the Pockels effect, (2) the Kerr effect.

Pockels Effect. For a given material, the application of an electric field E alters the dielectric permittivity tensor (nine components) in a linear fashion. A set of 27 components r_{ij} that satisfy the equation shown below completely determine these electro-optic coefficients:

$$\Delta(1/\epsilon_r)_i = r_{ij}E_j \tag{18}$$

Only certain components r_{ij} are large in magnitude and are exploited in practical applications. Typical r_{ij} values are from 1×10^{-12} m/V to 35×10^{-12} m/V; values for many ferroelectrics are given in Table 1. For example, in $LiNbO_3$, one of the ferroelectric oxides, $r_{33} = 3.08 \times 10^{-11}$ m/V (26). From Eq. (18), using $\epsilon_r = n^2$, one can obtain an expression for the change in refractive index, Δn, as

$$\Delta n = -\tfrac{1}{2}n^3 r_{33}E \tag{19}$$

Using $n = 2.29$ and $E = 10^6$ V/m, we have $\Delta n = 1.86 \times 10^{-4}$. This small change in the refractive index causes a change in the polarization of the material, leading to intensity modulation.

Kerr Effect. The quadratic electro-optic effect is also known as the Kerr effect. Here the change in refractive index is given as

$$\Delta n_{ij} = S_{ijkl}E_kE_l \tag{20}$$

The second-order coefficients S_{ijkl} are significantly enhanced when the energy of the optical signal is close to the bandgap energy of the material. In simple terms,

$$\Delta \mathbf{n} = -\tfrac{1}{2}\mathbf{g}n^3P^2 \tag{21}$$

where P is the magnitude of polarization, and $\mathbf{g}$, a fourth-rank tensor, is proportional to the S_{ijkl} of Eq. (20). For most materials the largest quadratic electro-optic effect is due to the difference between g_{11} and g_{12}. The quadratic electro-optic coefficients for various ferroelectrics are given in Table 4 (1).

Table 4. Quadratic Electro-Optic Coefficient $g_{11} - g_{12}$ for Various Polar Materials (1)

Material	$g_{11} - g_{12}$ ($m^4 \cdot C^{-2}$)
$BaTiO_3$	0.14
$LiNbO_3$	0.12
$LiTaO_3$	0.14
PLZT ceramics	0.010 to 0.018
$Ba_2NaNb_5O_{15}$	0.12
$SrTiO_3$	0.14
$K(TaNb)O_3$	0.16 to 0.20

Instead of the electric field dependence as shown in Eq. (20), the Kerr effect is easier to express in terms the intensity of light as (37)

$$n = n_0 + n_2I \tag{22}$$

where I is the intensity of the light, n_0 the refractive index without the light, and n_2 the refractive index due to the nonlinear effect. For waveguide modulation based on the Kerr effect an appropriate figure of merit is $n_2I/\lambda\alpha$, where λ is the wavelength and α the absorption coefficient. The Kerr effect is mostly observed in noncentrosymmetric crystals such as $AgGaS_2$, Ti_3AsSe_3, and polymers that contain asymmetric molecules.

Other Nonlinear Effects. The development of the laser has led to the study of nonlinear optics. Nonlinear light scattering, (e.g., Rayleigh, Brilliouin, and Raman scattering), though known before the advent of lasers, became more pronounced with the high intensity of the optical field of the laser. Third-order nonlinear effects are observed in centrosymmetric materials with high density of polarizable electrons. Hence, metals and organic molecules with extended electron wavelengths show strong third-order nonlinear effects (38). These materials find applications in liquid crystal displays, high-speed optical gates, real time holography, and optical transistors.

Acousto-Optic Effects

An acoustic wave propagating in a dielectric medium can introduce strain in the medium, causing variations in its refractive index. With this principle, acoustical holograms have been fabricated in display systems made of nematic liquid crystal panels. These devices are used in medical diagnostics. An acoustically tunable laser and acousto-optical amplifying tunable filter have been demonstrated using $LiNbO_3$ (Ref. 2, p. 328). This concept can be used in the modulation of an optical beam as well. A list of materials used for acousto-optic devices is found in Ref. 26, pp. 383–386.

OPTICAL COATINGS

Optical coatings or thin films of thickness 10 nm to 1000 nm deposited by evaporation or sputtering techniques in high-vacuum systems have wide applications. These applications include transparent conducting coatings, antireflective coatings, reflective coatings (cold light and heat mirrors), and a

Table 5. Physical Properties of Transparent Conducting Oxides (39)

Material	Electron Mobility ($cm^2/V \cdot s$)	Electron Carrier Concentration (cm^{-3})	Resistivity ($\Omega \cdot cm$)	Bandgap (eV)
CdO	2 to 120	5×10^{16} to 1×10^{21}	5×10^{-4}	2.3 to 2.7
Cd_2SnO_4	8 to 73	1×10^{17} to 1×10^{21}	5×10^{-4}	2.06 to 2.85
In_2O_3	15 to 70	1×10^{19} to 2×10^{21}	1×10^{-2} to 2×10^{-4}	3.6 to 3.85 (direct) 2.6 to (indirect)
SnO_2	10 to 50	1×10^{18} to 1×10^{21}	1×10^{-1} to 4×10^{-4}	3.97 to 4.63
ZnO	≈15	$\sim 5 \times 10^{20}$	$\approx 8 \times 10^{-4}$	3.3

variety of filters. Deposition process parameters such as the deposition rate, substrate temperature, and pressure during deposition significantly affect the microstructure (grain size, grain orientation, and grain morphology) of the thin films and hence the optical properties of the coatings. It is basically the electronic structure of the atoms or molecules that determines the optical properties of thin films. However, optical properties of thin films differ from those of bulk materials because of structural imperfections that dominate in thin films. These imperfections are voids, microcracks, pinholes, and dislocations. The transmittance T and reflectance R of these thin films are primarily determined by the refractive index n_f and the extinction coefficient k_f. Based on electromagnetic theory, expressions for T and R in terms of n_f and k_f are obtained in the following subsections.

Properties of Optical Coatings

For light incident from air or vacuum ($n = 1$) onto a partially absorbing film of thickness t, refractive index n_f and extinction coefficient k_f in contact with a thick, isotropic, weakly absorbing substrate with refractive n_s and extinction coefficient k_s, the coefficients T and R are given as (39)

$$T = \frac{16 n_s (n_f^2 + k_f^2)}{b_1 e^{\alpha} + b_2 e^{-\alpha} + b_3 \cos\eta + b_4 \sin\eta} \tag{23}$$

$$R = \frac{a_1 e^{\alpha} + a_2 e^{-\alpha} + a_3 \cos\eta + a_4 \sin\eta}{b_1 e^{\alpha} + b_2 e^{-\alpha} + b_3 \cos\eta + b_4 \sin\eta} \tag{24}$$

$$\alpha = 4\pi k_f t/\lambda, \qquad \eta = 4\pi n_f t/\lambda \tag{25}$$

The coefficients a_1, a_2, a_3, a_4, b_1, b_2, b_3, b_4 are essentially dependent on n_f, k_f, n_s, and k_s, and the algebraic expressions can be found in Ref. 40. The optical constants are strongly dependent on the wavelength, making the algebraic manipulation of Eqs. (23) and (24) quite difficult. However, some generalizations can be made. The index of refraction of most substrates is in the range of 1.4 to 1.6, and extinction coefficient is quite small (39). This results in negligible absorption by the substrate. Oxide films have higher refractive indices (≈2.0) and low extinction coefficients. These types of conditions lead to reflection being the dominant source of light loss.

Transparent Conducting Coatings

Transparent conducting oxides, or TCOs, are a special kind of materials that are transparent to visible light and conducting as well. However, their conductivities lie in between the conductivities of metals and dielectrics. Such materials include cadmium oxide (CdO), cadmium stannate (Cd_2SnO_4), indium oxide (In_2O_3), tin oxide (SnO_2), and zinc oxide (ZnO). These materials are also doped at cation sites with Sb, Cd, In, P, Te, Sn, Ti, or W and/or at anion sites with C1 or F to enhance their conductivities (39). Table 5 shows the physical properties of transparent conducting oxides (41). Indium oxide or indium oxide doped with tin (ITO) has been the material of choice for a variety of applications requiring transparent elec-

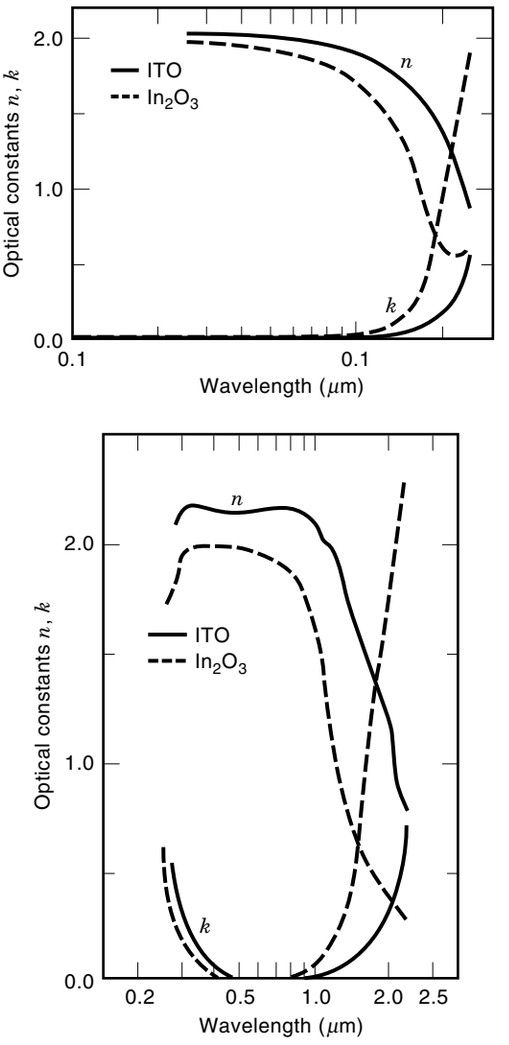

Figure 8. (a) Estimates of the refractive index and extinction coefficient for In_2O_3 and ITO; (b) measured refractive index and extinction coefficient for In_2O_3 and ITO (49)

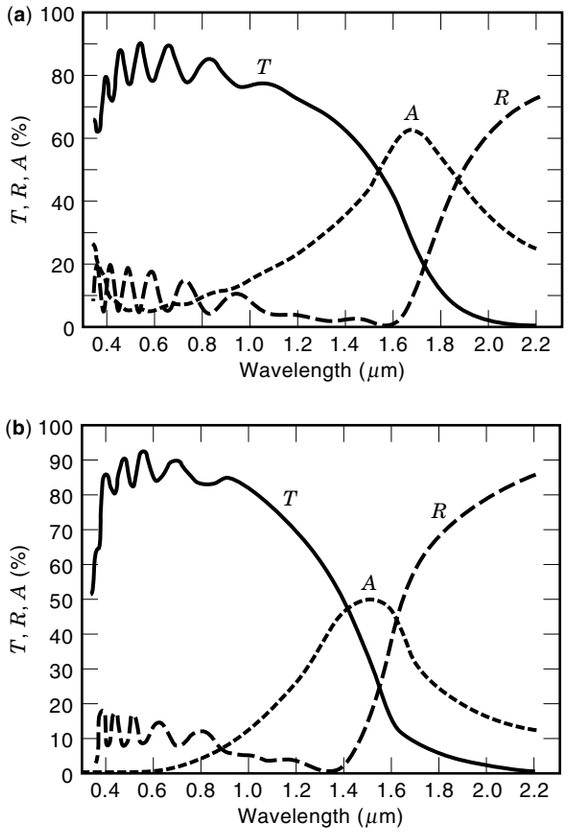

Figure 9. (a) Estimates of the transmission, reflection, and absorption of an ITO thin film; (b) published results on transmission, reflection, and absorption of spray-deposited ITO film (50)

trodes. The electrical and optical properties of ITO thin films have been investigated in detail to optimize simultaneously the conductivity and the transparency (40–42). Based on an *ab initio* Hartree–Fock calculation of the energy band diagram of In_2O_3 and ITO, an empirical relationship of the effective electron mass as a function of the ideal free carrier concentration is established (42). The importance of the varying electron effective mass in the prediction of complex dielectric function, the refractive index, extinction coefficient, and the optical transmittance based on Drude's theory is shown by comparing the estimated results with measured and published results (42). Figures 8(a) and (b) show the estimated and measured refractive index and extinction coefficient for In_2O_3 and ITO. Figure 9(a) shows estimates of the transmission, reflection, and absorption of an ITO film with the following properties: thickness 0.75 μm, carrier concentration 4.9×10^{20} cm^{-3}, electron effective mass $0.413m_0$, mobility 5.15 cm^2/V · s, resistivity $\approx 2.5 \times 10^{-4}$ $\Omega \cdot$ cm, and average transmittance 0.80 to 0.90 over wavelengths from 0.4 μm to 1.0 μm (40). These estimated results can be compared with the measured data shown in Fig. 9(b). The transmission and reflection are calculated using Eqs. (23) and (24). The absorption A is determined by the equation

$$A = 1 - T - R \tag{26}$$

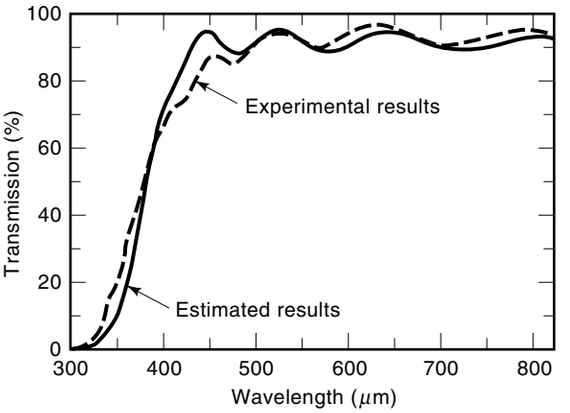

Figure 10. Measured and estimated transmission for an annealed ITO sample (44)

Figure 10 shows the measured and estimated transmission for an annealed ITO sample (40). The calculated figures of merit of ITO thin films based on estimates of transmission and conductivity are shown in Fig. 11 (43). The optimum carrier concentrations predicted from all figures of merit range from $\approx 6 \times 10^{20}$ cm^{-3} to $\approx 1.6 \times 10^{21}$ cm^{-3}. This range is well within the practical doping limits of ITO thin films (44). Recently, ITO thin films deposited on glass and polymer substrates by RF sputter deposition are characterized to correlate the sheet resistivity and transmission of these films with their microstructure (45).The refractive index and extinction coefficients are related to the microstructure of a thin film via the packing density, defined as the ratio of the volume of the solid part of the film (i.e., columns) to the total volume of the film (46). Typical values of packing density are 0.7 to 1.0 for optical films. The transmission and reflection are then related to the microstructure via n and k, using Eqs. (23) and (24). The refractive index n decreases with decreasing film density. The density is a function of the porosity of the material depending upon the content of solid material, e.g., grains and voids. Deposition process parameters such as substrate tem-

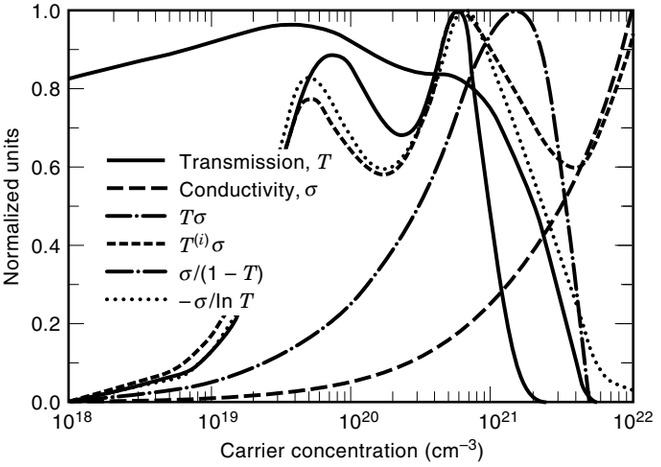

Figure 11. Calculation of the figures of merit of ITO thin films based on estimates of transmission and conductivity

Table 6. Optical Properties of Thin Films (50)

Material	Refractive Index	Transmittance Range (μm)
NaF	1.29 to 1.30	≥0.2
LiF	1.30	0.11 to 7
CaF_2	1.23 to 1.46	0.15 to 12
Na_3AlF_6	1.32 to 1.35	0.2 to 14
AlF_3	1.23	≥0.2
MgF_2	1.32 to 1.39	0.11 to 4
ThF_4	1.50	0.2 to 15
LaF_3	1.55	0.25 to 2
CeF_3	1.63	0.3 to 5
SiO_2	1.45 to 1.46	0.2 to 9
Al_2O_3	1.54	0.2 to 7
MgO	1.7	0.2 to 8
Y_2O_3	1.89	0.3 to 12
La_2O_3	1.98	≥0.3
CeO_2	2.2	0.4 to 12
ZrO_2	1.97	0.34 to 12
SiO	2.0	0.7 to 9
ZnO	2.1	≥0.4
TiO_2	1.9	0.4 to 3
ZnS	2.3	0.4 to 14
CdS	2.5	0.55 to 7
ZnSe	2.57	0.55 to 15
PbTe	5.6	3.5 to 20

perature and deposition rate affect the grain growth during e-beam or sputter deposition and need to be controlled carefully to maximize n and minimize k. The purity of the materials used and the cleanliness of the vacuum system affect the optical properties of thin films significantly (47).

Table 6 shows the optical properties of several thin film materials. Details on transparent conducting coatings can be found in Refs. 39 to 45, 47, 49, and 50. An excellent reference for optical properties of thin films is Ref. 48.

BIBLIOGRAPHY

1. J. C. Burfoot and G. W. Taylor, *Polar Dielectrics and their Applications,* Berkeley: University of California Press, 1979.
2. J. Saulnier, Lithium niobate for optoelectronic applications. In M. Quillec (ed.), *Materials for Optoelectronics,* Boston: Kluwer Academic, 1996.
3. M. E. Lines and A. M. Glass, *Principles and Applications of Ferroelectric Materials,* Oxford: Clarendon, 1977.
4. C. R. M. Grovenor, *Microelectronic Materials,* Adam Hilger, 1989.
5. J. Singh, *Optoelectronics,* New York: McGraw-Hill, 1996.
6. B. G. Streetman, *Solid State Electronic Devices,* 4th ed., Englewood Cliffs, NJ: Prentice-Hall, 1995.
7. M. A. Pollack, Advances in materials for optoelectronic and photonic integrated circuits, *Materials Sci. & Eng. B,* **B6**: 233–245, 1990.
8. S. M. Sze (ed.), *High Speed Semiconductor Devices,* New York: Wiley, 1990.
9. P. Bhattacharya, *Semiconductor Optoelectronic Devices,* Englewood Cliffs, NJ: Prentice-Hall, 1994.
10. S. M. Sze, *Physics of Semiconductor Devices,* 2nd ed., New York: Wiley, 1981.
11. R. M. Brody and V. J. Mazurczyk, In R. K. Willardson and A. C. Beer (eds.), *Semiconductors and Semimetals, 18,* New York: Academic, 1981.
12. H. Fritzsche, Noncrystalline semiconductors, *Phys. Today,* **37** (10): 34–43, 1984.
13. J. L. Stone, Photovoltaics: Unlimited electrical energy from the sun, *Phys. Today,* **46** (9): 22–31, 1993.
14. S. R. Forrest, Optoelectronic integrated circuits, *Proc. IEEE,* **75**: 1488–1497, 1987.
15. T. E. Bell, Electronics and the stars, *IEEE Spectrum,* **32** (8): 16–24, 1995.
16. C. Weisbuch, in R. Dingle (ed.), *Semiconductors and Semimetals, 24,* New York: Academic, 1987.
17. R. J. Collins, P. M. Fauchet, and M. A. Tischler, Porous silicon: From luminescence to LEDs, *Phys. Today,* **50** (1): 24–33, 1997.
18. *MRS Bull.,* **22** (2): 17–57, 1997.
19. T. P. Pearsall, Silicon/germanium optoelectronic materials. In M. Quillec (ed.), *Materials for Optoelectronics,* Boston: Kluwer Academic, 1996.
20. R. F. Davis, *Diamond Films and Coatings,* Park Ridge, NJ: Noyes Publications, 1993.
21. M. A. Capano and R. J. Trew, Silicon carbide electronic materials and devices, *MRS Bull.,* **22** (3): 19–24, 1997.
22. R. L. Gunshor, The wide band gap II–VI semiconductors. In M. Quillec (ed.), *Materials for Optoelectronics,* Boston: Kluwer Academic, 1996.
23. W. S. Ellis, Glass: Capturing the dance of light, *National Geographic,* **184** (6): 37–69, 1993.
24. S. Musikant, *Optical Materials,* New York: Marcel Dekker, 1985.
25. P. C. Becker and M. R. X de Barros, Optical fibers for telecommunications: Transmission and amplification. In M. Quillec (ed.), *Materials for Optoelectronics,* Boston: Kluwer Academic, 1996.
26. L. Solymar and D. Walsh, *Lectures on the Electrical Properties of Materials,* 4th ed., New York: Oxford University Press, 1988.
27. J. S. Sanghera and I. D. Aggarwal, *J. Non-crystalline Solids,* **213, 214**: 126–136, 1997.
28. J. Zarzyzki, *Glass and Vitreous State,* New York: Cambridge University Press, 1991.
29. S. P. Karna and A. T. Yeates, Nonlinear optical materials: Theory and modeling. In S. P. Karna and A. T. Yeates (eds.), *Nonlinear Optical Materials,* Washington, D.C.: American Chemical Society, 1996.
30. R. Levenson and J. Zyss, Polymer based optoelectronics from molecular optics to device technology. In M. Quillec (ed.), *Materials for Optoelectronics,* Boston: Kluwer Academic, 1996.
31. D. D. Nolte, *Photorefractive Effects and Materials,* Boston: Kluwer Academic, 1995.
32. Y. Yang, Polymer electroluminescent devices, *MRS Bull.,* **22** (6): 31–38, 1997.
33. T. Tsutsui, Progress in electroluminescent devices using molecular thin films, *MRS Bull.,* **22** (6): 39–45, 1997.
34. W. R. Slaneck and J. L. Bre'das, Conjugated polymer surfaces and interfaces for light-emitting devices, *MRS Bull.,* **22** (6): 46–51, 1997.
35. R. A. Colclaser and S. Diehl-Nagle, *Materials and Devices,* New York: McGraw-Hill, 1985.
36. L. C. Shen and J. A. Kong, *Applied Electromagnetism,* 3rd ed., Boston: PWS, 1995.
37. L. V. Aza'roff and J. J. Brophy, *Electronic Processes in Materials,* New York: McGraw-Hill, 1963.
38. D. Bloor, Nonlinear optical materials, an overview. In D. Bloor, R. J. Brook, M. C. Flemings, and S. S. Mahajan (eds.), *Encyclopedia of Advanced Materials,* New York: Pergamon, 1994.
39. J. L. Vossen, Transparent conducting films. In G. Hass, M. H. Francombe, and R. W. Hoffman (eds.), *Physics of Thin Films,* New York: Academic, 1977.

40. S. A. Knickerbocker and A. K. Kulkarni, Estimation and verification of the optical properties of indium tin oxide based on the energy band diagram, *J. Vac. Sci. Technol.,* **A14** (3): 757–761, 1996.
41. K. L. Chopra and S. R. Das, *Thin Film Solar Cells,* New York: Plenum, 1983.
42. A. K. Kulkarni and S. A. Knickerbocker, Estimation and verification of the electrical properties of indium tin oxide based on the energy band diagram, *J. Vac. Sci. Technol.,* **A14** (3): 1709–1713, 1996.
43. S. A. Knickerbocker and A. K. Kulkarni, Calculation of the figure of merit for indium tin oxide films based on basic theory, *J. Vac. Sci. Technol.,* **A13** (3): 1048–1052, 1995.
44. S. A. Knickerbocker, Estimation and verification of the electrical and optical properties of indium tin oxide based on the energy band diagram, Ph.D. Dissertation, Michigan Technological University, 1995.
45. A. K. Kulkarni et al., Electrical, optical and structural characteristics of indium tin oxide thin films deposited on glass and polymer substrates, *Thin Solid Films,* **308–309**: 1–7 (1997).
46. H. A. Macleod, Relationship of microstructure to optical properties of thin films, presented at *Topical Conference on Basic Optical Properties of Materials,* 1985.
47. T. S. Lim, Electrical, optical and structural properties of indium tin oxide thin films deposited on glass, PET and polycarbonate substrates by RF sputtering, M.S. Thesis, Michigan Technological University, 1997.
48. M. Ohring, *The Materials Science of Thin Films,* New York: Academic, 1992.
49. K. L. Chopra, S. Major, and D. K. Pandya, Transparent conductors: A status review, *Thin Solid Films,* **102**: 1–46, 1983.
50. T. Nagatomo, Y. Maruta, and O. Omoto, Electrical and optical properties of vacuum-evaporated indium–tin–oxide films with high electron mobility, *Thin Solid Films,* **192**: 17–25, 1990.

ANAND K. KULKARNI
Michigan Technological University